Review Article

High-resolution magnetic resonance imaging at 3T of pituitary gland: advantages and pitfalls

Marco Varrassi[1], Flavia Cobianchi Bellisari[2], Federico Bruno[2], Pierpaolo Palumbo[2], Raffaele Natella[3], Nicola Maggialetti[4], Massimo De Filippo[5], Ernesto Di Cesare[2], Antonio Barile[2], Carlo Masciocchi[2], Ferdinando Caranci[6], Alessandra Splendiani[2]

[1]Radiology Department, S. Salvatore Hospital, L'Aquila, Italy; [2]Department of Biotechnological and Applied Clinical Sciences, University of L'Aquila, L'Aquila, Italy; [3]Radiology Department, University of Campania "Luigi Vanvitelli", Naples, Italy; [4]Department of Life and Health "V. Tiberio", University of Molise, Campobasso, Italy; [5]Radiology Unit, University Hospital of Parma, Parma, Italy; [6]Neuroradiology Unit, University of Molise, Campobasso, Italy

Contributions: (I) Conception and design: A Splendiani, A Barile; (II) Administrative support: C Masciocchi, A Barile; (III) Provision of study materials or patients: A Splendiani, F Bruno; (IV) Collection and assembly of data: F Bruno, F Arrigoni, F Cobianchi Bellisari, N Maggialetti, R Natella; (V) Data analysis and interpretation: F Bruno, R Natella; (VI) Manuscript writing: All authors; (VII) Final approval of manuscript: All authors.

Correspondence to: Marco Varrassi. Division of Neuroradiology and Interventional Radiology, S. Salvatore Hospital, Via Vetoio, 1, 67100 L'Aquila, Italy. Email: mvarrassi27@yahoo.it.

Abstract: Magnetic resonance imaging (MRI) is the primary imaging tool for the evaluation of pituitary gland pathology. In the last decades, MRI with high-field scanners has become widely used in clinical practice, leading to significant improvements in image quality mainly thanks to a superior spatial resolution and signal intensity. Moreover, several advanced functional MRI sequences have been implemented for pituitary imaging, providing valuable information in diagnostic and presurgical planning of pituitary adenomas. Higher field strength presents however some technical pitfalls to be aware of. The purpose of this article is to review the state of the art of high-resolution MRI of the pituitary gland at 3 Tesla (3T), with a particular focus on the main benefits and the possible limitations of higher field imaging.

Keywords: Pituitary gland; magnetic resonance imaging (MRI); 3 Tesla (3T); spectroscopy; diffusion-weighted imaging (DWI)

Submitted Jan 21, 2019. Accepted for publication Jun 10, 2019.
doi: 10.21037/gs.2019.06.08
View this article at: http://dx.doi.org/10.21037/gs.2019.06.08

Introduction

Magnetic resonance imaging (MRI) is an accurate diagnostic tool with a primary indication in several condition both for a diagnostic and interventional intent (1-14). Notably, MRI has been established as dominant modality use in neuroradiological field due to its excellent soft tissue contrast (15-28), which allowed an accurate evaluation of intracranial structures. This characteristic proves to be particularly advantageous in the study of pituitary gland; MRI, indeed, provide a detailed depiction of the pituitary anatomy and its relationship with adjacent structures, helping from the detection of micro alteration of its architecture to the formulation of an adequate treatment planning. In this scenario, computed tomography (CT) take often only a complementary role in the study of pituitary gland, due to its lower soft tissue resolution than MR (11,29-35), useful therefore in identifying the presence of calcification, bony destruction, and surgically relevant bony anatomy (36-41). The purpose of this article is to review the state of the art of high-resolution MRI of the pituitary gland at 3 Tesla (3T), with a particular focus on the main benefits and the possible limitations of higher field imaging.

Anatomy and function of the pituitary gland

The hypophysis or pituitary gland lies in the sella turcica,

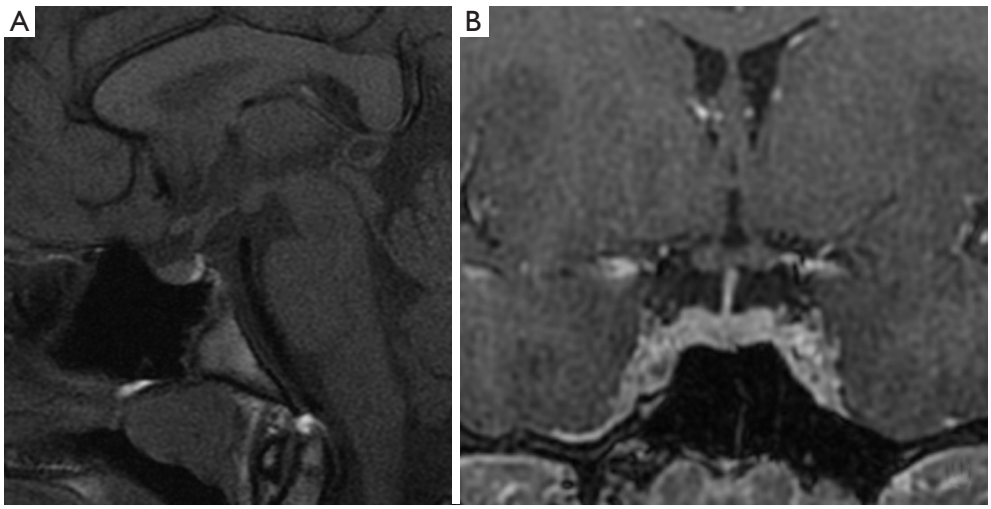

Figure 1 Sagittal T1 multi echo multiplanar (MEMP) spin-echo (SE), 3 mm slice thickness sequence (A) at 3T showing normal anatomy of the pituitary gland. Coronal 3D T1 fast spoiled gradient echo (FSPGR) 1 mm slice thickness sequence (B) after intravenous administration of gadolinium showing optimal visualization of the pituitary stalk and homogenous parenchymal enhancement.

a cup-shaped depression within the sphenoid bone. The pituitary gland is connected via the pituitary stalk to the hypothalamus which is a thin plate of tissue making up the floor of the anterior part of the 3rd ventricle.

The pituitary gland is formed by two distinct lobes, the anterior one known as adenohypophysis, and a posterior one kwon as neurohypophysis. Each lobe had a distinct embryological origin, considering that the anterior lobe forms from an invagination of the oral ectoderm known as Rathke's pouch and the posterior lobe develops from a protrusion of the neural ectoderm of the diencephalon.

The adenohypophysis is formed by three parts: pars tuberalis, pars intermedia and pars distalis. Different cell types are involved in hormones production, all involved in specific hormonal circuit which makes the adenohypophysis crucial in central regulation of several bodily function.

The neurohypophysis is divided into three parts: the posterior hypophysial (neural) lobe, the infundibular stem, and the median eminence. The posterior pituitary does not directly synthesize any hormones but instead releases some hormones synthesized in the hypothalamus and then released by exocytosis in the neural lobe. The functional state of the neural lobe is thus highly dependent upon the integrity of the pituitary stalk and hypothalamus (42).

Between the anterior and posterior lobes lies an intermediate lobe which is vestigial and known as the pars intermedia. This is a potential site for small non-functional Rathke's cyst (43). On both side of pituitary fossa there are the cavernous system, an anatomic compartment through which the internal carotid arteries enter the base, as well as the III, IV, VI cranial nerves, and first and second branches of the V cranial nerve exit the skull.

MRI technique and imaging protocol

MR protocol study requires sagittal and coronal planes, both in thin sections (2 or 3 mm), focused on the pituitary. It is necessary to perform T1-weighted sequences before and after administration of intravenous contrast. Coronal T2-weighted sequences can add some information, but they result less sensitive in the assessing of adenomas. Plans are obtained with specific orientations. The sagittal plane should be oriented parallel to the bi-hemispheric line from a coronal plane. The coronal plane is obtained from a sagittal plane, parallel to the hypophyseal pedicle (*Figure 1*). It is important to perform post-contrast MR sequences in a dynamic modality (within 40–50 seconds after contrast injection there is a homogenous enhancement of the gland). In this way it is possible to highlight adenomas, as they typically enhance less than the normal pituitary tissue, due to the presence of hypophyseal portal system, and this differential enhancement is sometimes best appreciated within the first arterial phase of the contrast injection. Most of the pituitary adenomas, on the contrary, receive a direct extra portal arterial supply. In the majority of cases, however, lesions are adequately demonstrated on a standard

acquisition (non-dynamic) after contrast administration (44).

Microadenomas (diameter <1 cm) can be detected with additional dynamic sagittal plane images to the routine coronal planes (*Figure 2*) (45). Dynamic contrast MRI also has an equally important role in studying macroadenomas (diameter ≥1 cm) (*Figure 3*), in cases of possible invasion of the cavernous sinus, and in assessing residual/recurrent tumor from postoperative tissues (46). Some microadenomas exhibit maximum lesion-to-gland contrast on unenhanced scan; however, this image contrast begins to diminish the moment the contrast-enhancing agent arrives in the pituitary gland. It is important to remind that the pituitary gland, pituitary stalk and cavernous sinuses are all vascular structures which enhance after gadolinium injection, the optic chiasm and hypothalamus, on the other hand, do not show enhancement if the blood-brain barrier is intact.

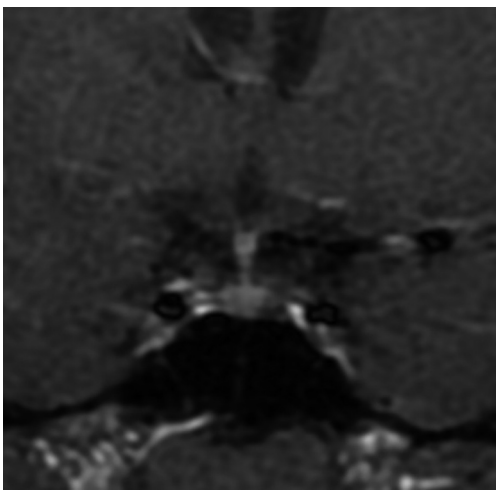

Figure 2 Coronal T1 spin-echo (SE) sequence after dynamic contrast enhancement at 3T scanner showing a 3 mm area of delayed enhancement in the left portion of adenohypophysis, consistent with microadenoma.

Higher resolution pituitary images can be provided by the use of high field strength 3T MR scanners. 3T MRI, thanks to a higher magnetic field than 1.5 Tesla (1.5T) allows to improve image quality and spatial resolution, which are fundamental especially in evaluating subtle differences between normal and abnormal tissue. The superiority of high field scanner at 3T MRI to 1.5T have been demonstrated in several studies.

Kim *et al.* (47) showed that preoperative localization of pituitary microadenomas in Cushing's disease is better with 3T MRI compared to 1.5T MRI, although some of these lesions were missed.

They conducted a preliminary study, depicting how 3T MRI can be useful in the evaluation algorithm for Cushing's disease, amplifying radiographic differences when a subtle imaging abnormality exists. If MRI at 3T plays a central role in the clinical diagnostic field, it revealed to be more

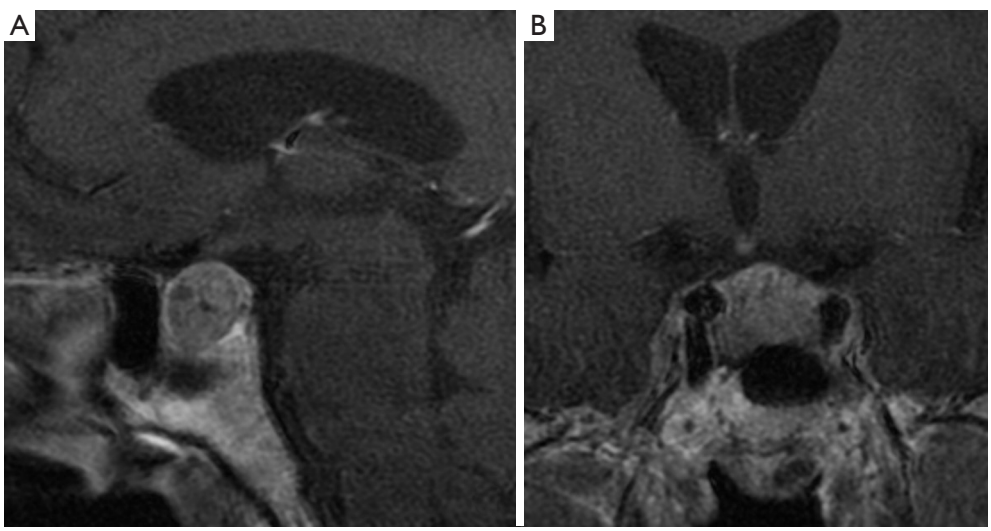

Figure 3 Sagittal T1 multi echo multiplanar (MEMP) spin-echo (SE) 3 mm slice thickness sequence (A) and coronal T1 MEMP SE 3 mm slice thickness (B) at 3T scanner, both performed after administration of contrast medium, showing inhomogeneous solid mass involving sellar and suprasellar region causing mild displacement of optic chiasm, likely referable to macroadenoma.

Figure 4 Axial T1 fat-suppressed fast spoiled gradient echo (FSPGR) 1 mm slice thickness sequence after administration of contrast medium at 3T scanner, showing pathological enhancement involving right orbital apex and anterior aspect of ipsilateral cavernous sinus, encasing the intracanalicular portion of optic nerve. A case of Tolosa-Hunt syndrome.

accurate than 1.5T also in neurosurgical procedures and gamma knife, stereotactic radiosurgery (SRS) or stereotactic radiotherapy (SRT) planning.

Pinker *et al*. (48) conducted a study assessing the value of high-field MRI for both diagnosis and surgery of sellar lesions, predicting tumor invasion through the medial cavernous sinus border.

In another study, Fahlbusch and Buchfelder (49) observed that up to 10% of pituitary adenomas infiltrate into parasellar spaces. To assess parasellar spaces invasion is fundamental in surgery planning, as it represents the most common limiting factor in the resection of pituitary adenomas; standard field 1.5T MRI rarely allows to delineate the medial limit of the cavernous sinus and the possible extension into the parasellar spaces. High field 3T MRI scan has been found to be superior to conventional MR units in delineation of parasellar anatomy (*Figure 4*), defining medial cavernous sinus border. What is more, 3T MRI offers a better depiction of the intracavernous cranial nerves and optic chiasm. Satogami *et al.* used high resolution MRI at 3T to evaluate the normal pituitary stalk in detail, thereby providing a standard for size of the normal pituitary stalk. It is fundamental starting from the knowledge of the normal imaging appearance of the pituitary stalk in order to make an accurate diagnosis of pituitary infundibular lesions. On high-resolution T2-weighted images, pituitary stalk is characterized by a central hyperintensity and a peripheral rim of isointensity which may represent the infundibular stem and pars tuberalis respectively (50).

Magnetization transfer (MT) imaging is a recent technique that can play a central role in evaluating preoperative and postoperative pituitary adenomas in patients with hyperprolactinemia. In fact, in this imaging modality, the tissue contrast depends mainly on the concentration of macromolecules and quantified by the MT ratio (MTR). Thanks to this modality, it is possible to make difference between prolactin-secreting adenomas and the non-secreting ones. This technique is also important in post-operative assessment and follow-up of patients with pituitary adenomas, as an increased MTR is strongly suggestive of a residual tumor, even if standard MR results negative (51).

Diffusion-weighted imaging (DWI) and apparent diffusion coefficient (ADC) maps result crucial in defining tumor component and consistency. Describing tissue characteristics is important, as a soft microadenoma should be easily removed with a minimally invasive endoscopic trans-sphenoidal access, avoiding invasive surgery; on the other hand, 10% of macroadenomas presenting a high percentage of fibrosis needs a surgical invasive approach. In this scenario it is easily to understand how the definition of macroadenomas consistency plays a central role in planning an adequate surgical technique for resection. Several studies attempted to predict adenoma consistency by using conventional and some novel MRI sequences with controversial results, especially regarding DWI. In fact, this sequence has shown utility in assessing the consistency of adenomas (52-54), but with no convincing data, due to the B_0 related artifacts in the sellar region (55-57). Yiping *et al*. (58) used the BLADE DWI sequence to acquire ADC values, which reduced artefacts in the sellar region and enhanced the accuracy of signal. BLADE DWI is a turbo spin echo-based diffusion-weighted technique that can oversample the region in the centre on the k-space to correct for heterogeneities prior to combing data. Using this approach they revealed that ADC ratio decreased with increasing collagen content and predicted hard consistency of tumors for ADC <1.077.

Proton magnetic resonance spectroscopy (1H-MRS) is a MR-based technique able to measure concentrations of different metabolites in the cerebral parenchima, widely used for differentiating neoplastic from non-neoplastic

pathology. In fact this method allows to define tumor type, grade, proliferation and to predict therapeutic sensitivity and prognosis in different central nervous system pathologies (59). The application of 1H-MRS in the sellar region is found as a diagnostic tool in the evaluation of sellar and parasellar neoplasms. It has been shown that hypothalamic gliomas, for example, are defined by increased choline and decreased N-acetyl aspartate peaks, while pituitary adenomas may show only an increase of choline peak or no metabolites if there is an intramural haemorrhage, as iron ions of hemosiderin lead to worsened homogeneity of the magnetic field (60). Hypothalamic hamartomas show decreased N-acetyl aspartate and increased myo-inositol compared to grey matter (61). Craniopharyngiomas and germinomas are defined by a dominant lipid peak (62,63). Hu *et al*. enhanced the capability of 1H-MRS in predicting the pathological subtype and somatostatin receptor 2 (SSTR2) expression of growth hormone-secreting pituitary adenomas (GH-PAs). In fact, the best medical treatment of acromegaly after surgery is somatostatin analogs (SSAs); however, one-third of patients show some degree of resistance to SSA treatment. In this scenario, it is crucial to identify factors that could be related to resistance to SSA therapy. 1H-MRS may be a useful, non-invasive method to predict tumor subtype and SSTR2 expression. One of the best predictors, among the several parameters of MRS, is considered to be the choline/creatine (Ch/Cr) ratio. This value has revealed to be consistent with others reported predictors of SSA response, such as T2 signal intensity and the Ki-67 value. MRS could have also a role in predicting subtype in cases of isointense T2 signals. In this way, MRS could represent a potentially novel and non-invasive method to predict the response to SSAs in patients with GH pituitary macroadenomas (64).

Another field in which 3T MRI scan showed to be fundamental is the intraoperative navigation.

Wolfsberger *et al*. (65) decided to do intraoperative navigation guided combining 3T MR images with CT scans; in this case, CT scans plays a role during trans-sphenoidal approach to depict the nasal bone structures, while 3T MRI scans result particularly useful to explore parasellar tumor extension during microsurgical and/or endoscopic resection. Nakazawa *et al*. (66) determined how 3T is superior to 1.5T for sellar lesions with small pituitary tumors; 3T is better than 1.5T to differentiate tumor and normal tissue in SRS and SRT planning of pituitary tumors. What is more, they showed that for both field strengths, three dimensional-fast spoiled gradients recalled acquisition in the steady state (3D-FSPGR) enabled the high-resolution acquisition, and two-dimensional spin-echo (SE) T1-weighted (2D-T1W1) and 2D-fluid-attenuated inversion recovery (FLAIR) were able to well enhance tissue contrast (66).

Pitfalls

Although the cited benefits, the high magnetic field of 3T scanner is related to some limits which is mandatory to take into account for a comprehensive evaluation of 3T pituitary study.

It is well known, indeed, that susceptibility effects increase with higher B_0, as well as artifacts related to vascular flow and patient movement are more pronounced and sometimes may outweigh the benefits, even 3T shows an increased capability in the detection of microbleeds in vascular encephalopathy.

Besides, problems with specific absorption ratio (SAR) limitations are correlated with an increase in field strength. Although even small reductions of the flip angle lead to significant SAR decreases, flip angle reductions may cause a reduction in signal intensity, limiting the gain from higher fields. The use of gradient echo sequences is a valuable alternative, even if these sequences are prone to susceptibility artifacts which limit their use (67).

Lastly, grey-to-white matter contrast is reduced in SE T1 imaging at 3T when compared to 1.5T, since T1 times of grey and white matter lengthen and converge at higher fields. Inversion recovery sequences provide a superior grey-to-white matter contrast but, on the other hand, enhancing lesions may not be visible. Therefore, these sequences are not quite useful for comparative pre- and postcontrast imaging, regardless of B_0 (68).

Conclusions

MRI represent the mainstay imaging modality nowadays in the evaluation of both pituitary gland and sellar and parasellar structures thanks to its excellent contrast resolution and the possibility to obtain a dynamic evaluation of contrast enhancement within the pituitary tissue, which represents a critical factor in the detection of pituitary adenomas.

High field 3T-MRI, despite some limitations, mainly regarding increased SAR exposure, changes in T1 relaxation times and susceptibility effects, can provide several advantages over 1.5T scanners, ranging from a higher spatial resolution to the possibility of acquiring dedicated

MRI sequences (e.g., BLADE DWI sequences). Also, 3T-MRI enables a more accurate evaluation of important parameters of pituitary adenomas such as composition and consistency and provides crucial elements helping in the differential diagnosis of a wide range of neoplasms which may affect sellar and parasellar region thanks to MRS applications.

Acknowledgments

None.

Footnote

Conflicts of Interest: The authors have no conflicts of interest to declare.

Ethical Statement: The authors are accountable for all aspects of the work in ensuring that questions related to the accuracy or integrity of any part of the work are appropriately investigated and resolved.

References

1. Mariani S, La Marra A, Arrigoni F, et al. Dynamic measurement of patello-femoral joint alignment using weight-bearing magnetic resonance imaging (WB-MRI). Eur J Radiol 2015;84:2571-8.
2. Cazzato RL, Arrigoni F, Boatta E, et al. Percutaneous management of bone metastases: state of the art, interventional strategies and joint position statement of the Italian College of MSK Radiology (ICoMSKR) and the Italian College of Interventional Radiology (ICIR). Radiol Med 2019;124:34-49.
3. Mattera M, Reginelli A, Bartollino S, et al. Imaging of metabolic bone disease. Acta Biomedica 2018;89:197-207.
4. Bruno F, Barile A, Arrigoni F, et al. Weight-bearing MRI of the knee: A review of advantages and limits. Acta Biomed 2018;89:78-88.
5. Arrigoni F, Bruno F, Zugaro L, et al. Role of interventional radiology in the management of musculoskeletal soft-tissue lesions. Radiol Med 2019;124:253-8.
6. Barile A, Arrigoni F, Bruno F, et al. Present role and future perspectives of interventional radiology in the treatment of painful bone lesions. Future Oncol 2018;14:2945-55.
7. Masciocchi C, Conti L, D'Orazio F, et al. Errors in musculoskeletal MRI. In: Romano L, Pinto A. editors. Errors in Radiology. Springer-Verlag, Milan 2012:209-17.
8. Masciocchi C, Barile A, Lelli S, et al. Magnetic Resonance Imaging (MRI) and arthro-MRI in the evaluation of the chondral pathology of the knee joint. Radiol Med 2004;108:149-58.
9. Ferrari F, Arrigoni F, Miccoli A, et al. Effectiveness of Magnetic Resonance-guided Focused Ultrasound Surgery (MRgFUS) in the uterine adenomyosis treatment: technical approach and MRI evaluation. Radiol Med 2016;121:153-61.
10. Barile A, Arrigoni F, Zugaro L, et al. Minimally invasive treatments of painful bone lesions: state of the art. Med Oncol 2017;34:53.
11. Barile A, Arrigoni F, Bruno F, et al. Computed Tomography and MR Imaging in Rheumatoid Arthritis. Radiol Clin North Am 2017;55:997-1007.
12. Reginelli A, Zappia M, Barile A, et al. Strategies of imaging after orthopedic surgery. Musculoskelet Surg 2017;101:1.
13. Barile A, Regis G, Masi R, et al. Musculoskeletal tumours: preliminary experience with perfusion MRI. Radiol Med 2007;112:550-61.
14. Barile A, Lanni G, Conti L, et al. Lesions of the biceps pulley as cause of anterosuperior impingement of the shoulder in the athlete: potentials and limits of MR arthrography compared with arthroscopy. Radiol Med 2013;118:112-22.
15. Splendiani A, Puglielli E, De Amicis R, et al. Spontaneous resolution of lumbar disk herniation: Predictive signs for prognostic evaluation. Neuroradiology 2004;46:916-22.
16. Barile A, Limbucci N, Splendiani A, et al. Spinal injury in sport. Eur J Radiol 2007;62:68-78.
17. Perri M, Grattacaso G, di Tunno V, et al. T2 shine-through phenomena in diffusion-weighted MR imaging of lumbar discs after oxygen-ozone discolysis: a randomized, double-blind trial with steroid and O2-O3 discolysis versus steroid only. Radiol Med 2015;120:941-50.
18. Perri M, Grattacaso G, Di Tunno V, et al. MRI DWI/ADC signal predicts shrinkage of lumbar disc herniation after O2-O3 discolysis. Neuroradiol J 2015;28:198-204.
19. Marsecano C, Bruno F, Michelini G, et al. Systemic metastases from central nervous system ependymoma: Case report and review of the literature. Neuroradiol J 2017;30:274-80.
20. Splendiani A, Perri M, Grattacaso G, et al. Magnetic resonance imaging (MRI) of the lumbar spine with dedicated G-scan machine in the upright position: a retrospective study and our experience in 10 years with 4305 patients. Radiol Med 2016;121:38-44.

21. Splendiani A, Perri M, Marsecano C, et al. Effects of serial macrocyclic-based contrast materials gadoterate meglumine and gadobutrol administrations on gadolinium-related dentate nuclei signal increases in unenhanced T1-weighted brain: a retrospective study in 158 multiple sclerosis (MS) patients. Radiol Med 2018;123:125-34.
22. Gallucci M, Limbucci N, Zugaro L, et al. Sciatica: treatment with intradiscal and intraforaminal injections of steroid and oxygen-ozone versus steroid only. Radiology 2007;242:907-13.
23. Splendiani A, Ferrari F, Barile A, et al. Occult neural foraminal stenosis caused by association between disc degeneration and facet joint osteoarthritis: Demonstration with dedicated upright MRI system. Radiol Med 2014;119:164-74.
24. Patriarca L, Letteriello M, Di Cesare E, et al. Does evaluator experience have an impact on the diagnosis of lumbar spine instability in dynamic MRI? Interobserver agreement study. Neuroradiol J 2015;28:341-6.
25. Splendiani A, Bruno F, Patriarca L, et al. Thoracic spine trauma: advanced imaging modality. Radiol Med 2016;121:780-92.
26. Michelini G, Corridore A, Torlone S, et al. Dynamic MRI in the evaluation of the spine: State of the art. Acta Biomed 2018;89:89-101.
27. Splendiani A, Bruno F, Mariani S, et al. A rare localization of pure dermoid cyst in the frontal bone. Neuroradiol J 2016;29:130-3.
28. Bruno F, Smaldone F, Varrassi M, et al. MRI findings in lumbar spine following O2-O3 chemiodiscolysis: A long-term follow-up. Interv Neuroradiol 2017;23:444-50.
29. Barile A, Bruno F, Arrigoni F, et al. Emergency and Trauma of the Ankle. Semin Musculoskelet Radiol. 2017;21:282-9.
30. Barile A, Reginelli F, De Filippo M, et al. Diagnostic imaging and intervention of the musculoskeletal system: state of the art. Acta Biomed 2018;89:5-6.
31. Duyn JH, van Gelderen P, Li TQ, et al. High-field MRI of brain cortical substructure based on signal phase. Proc Natl Acad Sci 2007;104:11796-801.
32. Chalela JA, Kidwell CS, Nentwich LM, et al. Magnetic resonance imaging and computed tomography in emergency assessment of patients with suspected acute stroke: a prospective comparison. Lancet 2007;369:293-8.
33. Boas FE, Fleischmann D. CT artifacts: Causes and reduction techniques. Imaging Med 2012;4:229-40.
34. Di Pietto F, Chianca V, de Ritis R, et al. Postoperative imaging in arthroscopic hip surgery. Musculoskelet Surg 2017;101:43-9.
35. De Filippo M, Pesce A, Barile A, et al. Imaging of postoperative shoulder instability. Musculoskelet Surg 2017;101:15-22.
36. Di Cesare E, Splendiani A, Barile A, et al. CT and MR imaging of the thoracic aorta. Open Med (Wars) 2016;11:143-51.
37. Floridi C, Reginelli A, Capasso R, et al. Percutaneous needle biopsy of mediastinal masses under C-arm conebeam CT guidance: diagnostic performance and safety. Med Oncol 2017;34:67.
38. Arrigoni F, Barile A, Zugaro L, et al. CT-guided radiofrequency ablation of spinal osteoblastoma: treatment and long-term follow-up. Int J Hyperthermia 2018;34:321-7.
39. Di Cesare E, Patriarca L, Panebianco L, et al. Coronary computed tomography angiography in the evaluation of intermediate risk asymptomatic individuals. Radiol Med 2018;123:686-94.
40. Lundin P, Bergström K, Thuomas KA, et al. Comparison of MR imaging and CT in pituitary macroadenomas. Acta Radiol 1991;32:189-96.
41. Di Cesare E, Gennarelli A, Di Sibio A, et al. Assessment of dose exposure and image quality in coronary angiography performed by 640-slice CT: a comparison between adaptive iterative and filtered back-projection algorithm by propensity analysis. Radiol Med 2014;119:642-9.
42. Elster AD. Imaging of the sella: Anatomy and pathology. Semin Ultrasound CT MR 1993;14:182-94.
43. Evanson EJ. Imaging the pituitary gland. Imaging 2002;14:93-102.
44. Bonneville JF, Bonneville F, Cattin F. Magnetic resonance imaging of pituitary adenomas. Eur Radiol 2005;15:543-8.
45. Gao R, Isoda H, Tanaka T, et al. Dynamic gadolinium-enhanced MR imaging of pituitary adenomas: Usefulness of sequential sagittal and coronal plane images. Eur J Radiol 2001;39:139-46.
46. Yuh WT, Fisher DJ, Nguyen HD, et al. Sequential MR enhancement pattern in normal pituitary gland and in pituitary adenoma. AJNR Am J Neuroradiol 1994;15:101-8.
47. Kim LJ, Lekovic GP, White WL, et al. Preliminary Experience with 3-Tesla MRI and Cushing's Disease. Skull Base 2007;17:273-7.
48. Pinker K, Ba-Ssalamah A, Wolfsberger S, et al. The value of high-field MRI (3T) in the assessment of sellar lesions. Eur J Radiol 2005;54:327-34.
49. Fahlbusch R, Buchfelder M. Recurrent Pituitary Adenomas. In: Samii M. editor. Surgery of the Sellar

Region and Paranasal Sinuses. Berlin, Heidelberg: Springer, 1991:251-66.
50. Satogami N, Miki Y, Koyama T, et al. Normal pituitary stalk: High-resolution MR imaging at 3T. Am J Neuroradiol 2010;31:355-9.
51. Argyropoulou MI, Kiortsis DN. Magnetization transfer imaging of the pituitary gland. Hormones (Athens) 2003;2:98-102.
52. Boxerman JL, Rogg JM, Donahue JE, et al. Preoperative MRI Evaluation of Pituitary Macroadenoma: Imaging Features Predictive of Successful Transsphenoidal Surgery. AJR Am J Roentgenol 2010;195:720-8.
53. Mahmoud OM, Tominaga A, Amatya VJ, et al. Role of PROPELLER diffusion weighted imaging and apparent diffusion coefficient in the diagnosis of sellar and parasellar lesions. Eur J Radiol 2010;74:420-7.
54. Mohamed FF, Abouhashem S. Diagnostic value of apparent diffusion coefficient (ADC) in assessment of pituitary macroadenoma consistency. Magn Reson Med 2002;47:42-52
55. Pipe JG, Farthing VG, Forbes KP. Multishot diffusion-weighted FSE using PROPELLER MRI. Magn Reson Med 2002;47:42-52.
56. Suzuki C, Maeda M, Hori K, et al. Apparent diffusion coefficient of pituitary macroadenoma evaluated with line-scan diffusion-weighted imaging. J Neuroradiol 2007;34:228-35.
57. Kumazawa S, Ushijima D, Yabuuchi H. Changes of the apparent diffusion coefficient in brain diffusion-weighted images due to subject positioning: A simulation study. J Neuroradiol 2015;42:150-5.
58. Yiping L, Ji X, Daoying G, et al. Prediction of the consistency of pituitary adenoma: A comparative study on diffusion-weighted imaging and pathological results. J Neuroradiol 2016;43:186-94.
59. Law M, Yang S, Wang H, et al. Glioma Grading: Sensitivity, Specificity, and Predictive Values of Perfusion MR Imaging and Proton MR Spectroscopic Imaging Compared with Conventional MR Imaging. AJNR Am J Neuroradiol 2003;24:1989-98.
60. Stadlbauer A, Buchfelder M, Nimsky C, et al. Proton magnetic resonance spectroscopy in pituitary macroadenomas: preliminary results. J Neurosurg 2008;109:306-12.
61. Freeman JL, Coleman LT, Wellard RM, et al. MR Imaging and Spectroscopic Study of Epileptogenic Hypothalamic Hamartomas: Analysis of 72 Cases. Am J Neuroradiol 2004;25:450-62.
62. Sutton LN, Wang ZJ, Wehrli SL, et al. Proton spectroscopy of suprasellar tumors in pediatric patients. Neurosurgery 1997;41:388-94.
63. Kendi TK, Çaglar S, Huvaj S, et al. Suprasellar germ cell tumor with subarachnoid seeding: MRI and MR spectroscopy findings. Clin Imaging 2004;28:404-7.
64. Hu J, Yan J, Zheng X, et al. Magnetic resonance spectroscopy may serve as a presurgical predictor of somatostatin analog therapy response in patients with growth hormone-secreting pituitary macroadenomas. J Endocrinol Invest 2019;42:443-51.
65. Wolfsberger S, Ba-Ssalamah A, Pinker K, et al. Application of three-tesla magnetic resonance imaging for diagnosis and surgery of sellar lesions. J Neurosurg 2004;100:278-86.
66. Nakazawa H, Shibamoto Y, Tsugawa T, et al. Efficacy of magnetic resonance imaging at 3 T compared with 1.5 T in small pituitary tumors for stereotactic radiosurgery planning. Jpn J Radiol 2014;32:22-9.
67. Pattany PM. 3T MR imaging: The pros and cons. AJNR Am J Neuroradiol 2004;25:1455-6.
68. Schmitz BL, Aschoff AJ, Hoffmann MH, et al. Advantages and pitfalls in 3T MR brain imaging: A pictorial review. Am J Neuroradiol 2005;26:2229-37.

Cite this article as: Varrassi M, Cobianchi Bellisari F, Bruno F, Palumbo P, Natella R, Maggialetti N, De Filippo M, Di Cesare E, Barile A, Masciocchi C, Caranci F, Splendiani A. High-resolution magnetic resonance imaging at 3T of pituitary gland: advantages and pitfalls. Gland Surg 2019;8(Suppl 3):S208-S215. doi: 10.21037/gs.2019.06.08

